Polymer Vol. 39 No. 25, pp. 6429–6439, 1998

0032-3861/98/$ - see front matter

PII: S0032-3861(98)00035-4

Polystyrene/poly(2-vinyl pyridine) heteroarm star copolymer micelles in toluene: morphology and thermodynamics†

D. Voulgaris[a], C. Tsitsilianis[a,*], F. J. Esselink[b] and G. Hadziioannou[b]
[a]*Department of Chemical Engineering, University of Patras, and Institute of Chemical Engineering and High Temperature Chemical Processes, ICE/HT-FORTH, P.O. Box 1414, 26500 Patras, Greece*
[b]*Department of Polymer Chemistry and Materials Science Center, University of Groningen, Nijenborgh 4, 9747 AG Groningen, The Netherlands*
(Accepted 16 December 1997)

Polystyrene/poly(2-vinyl pyridine) heteroarm star copolymer (i.e. star-shaped polymers consisting of a central poly(divinyl benzene) core bearing an equal number of polystyrene and poly(2-vinyl pyridine) arms, PS_6P2VP_6) and the corresponding diblock copolymer were investigated in toluene, which is a selective solvent for PS. The star copolymers are associated in polymolecular micelles following the closed association model. The characteristics of micelles were determined by means of static light scattering, viscometry and cryo-transmission electron microscopy. The micelles adopt a core-shell structure of spherical shape with core radius almost equal to the corona thickness. Comparing their solution behaviour with that of the corresponding diblock copolymer, having the same block lengths as those of the star arms, significant differences were observed. The A_nB_n exhibit *cmc* which is three orders of magnitude higher and an aggregation number which is about one order of magnitude lower with respect to the AB copolymer. The thermodynamics of micellization were also studied. ΔG^0, ΔH^0 and ΔS^0 were found to be negative for both systems. ΔG^0 is less negative for the star copolymer implying a smaller driving force for micellization. This is due to a pronounced loss of the combinatorial entropy of the star polymer arms.

(Keywords: heteroarm star copolymer; micelle; cryo-transmission electron microscopy)

INTRODUCTION

Star-shaped macromolecules have been widely used as model branched polymers attempting to evaluate the influence of segment density and chain topology on the properties of polymers[1,2]. In recent years we have developed a synthetic route in order to prepare star-shaped block copolymers named heteroarm star copolymers. These polymeric species consist of a central poly(divinyl benzene) core bearing two kinds of chemically different arms of the type A_nB_n[3–5]. They can be viewed as a number of diblock copolymers joined together at their A–B junction points (*Scheme 1*).

Their synthesis relies on sequential anionic 'living' copolymerization and comprises three steps. In the first step a living polymer precursor is formed, which is subsequently used to initiate the polymerization of a small amount of divinylbenzene (second step). A 'living' star-shaped polymer is formed bearing within its core a number of active sites that are equal to the number of its arms. In the third step these active sites initiate the polymerization of a new incoming monomer yielding the second generation of the arms. This procedure provides symmetry on the number of the heteroarms.

It is well established that block copolymers form supramolecular assemblies through macromolecular association in a selective solvent[6–9]. The so-formed block copolymer micelles exhibit a core-shell structure where the better solubilized parts constitute the shell or the corona and the insoluble or worse solubilized parts constitute the core. The phenomenon of the polymer micellization in most cases follows the closed association model according to which, above a certain concentration called the 'critical micelle concentration' (*cmc*) the macromolecules start to form polymolecular micelles. The *cmc* and the micelle features such as aggregation number, core and corona size and shape are governed by a number of factors such as the selectivity of the solvent, the molecular characteristics of the copolymer (i.e. molecular weight, composition, architecture) and the temperature.

Recently we have reported some preliminary results concerning association phenomena of heteroarm star copolymers in selective solvents. Amphiphilic polystyrene–poly(ethylene oxide) star A_nB_n type block copolymers form micelles in water as well as in tetrahydrofuran[10]. Analogous behaviour was also observed in the polystyrene/poly(*t*-butyl acrylate)(PS_nPtBA_n)–methanol system[11].

In the present article a detailed study of the association phenomena exhibited by such novel star-shaped copolymers is reported. The system chosen was polystyrene/poly(2-vinyl pyridine) (PS_nP2VP_n)[12] in toluene. A number of articles dealing with linear block copolymers (i.e. diblock and triblock) have already appeared in the literature showing that micellization phenomena take place due to the association of the insoluble P2VP blocks of the copolymers[13–15]. The system offers some experimental advantages concerning static light scattering and transmis-

* To whom correspondence should be addressed
† Part of this work was presented at the 17th 'Hellenic Conference on Chemistry' held in Patras, Greece, December 1996

sion electron microscopy. In the former case the refractive index increments of the copolymer constituents, PS and P2VP, in toluene are very close and therefore possible chemical heterogeneity of the samples does not affect the determination of the aggregation numbers. In the latter case cryo-electron microscopy, an experimental tool recently applied to block copolymer solutions, can be used. As has been reported recently morphologies of PS-b-P2VP diblock copolymers micelles dissolved in toluene can be visualized in dissolved state by means of cryo-transmission electron microscopy[16,17]. This technique permits the study of frozen 'solutions' of a synthetic polymer in a volatile organic solvent like toluene which remains amorphous in the frozen state.

In the system investigated here, the critical micelle concentration was detectable by static light scattering experiments. By determining *cmc* values as a function of temperature and observing that the micellization phenomena of the star copolymer meet the closed association model, the standard thermodynamic quantities (ΔG^0, ΔH^0 and ΔS^0) of micellization could be calculated.

In order to evaluate the effect of the star-shaped architecture on the micellization phenomena, a linear diblock copolymer PS-b-P2VP was involved in the present study. This copolymer exhibits similar P2VP content compared with the star copolymer and its blocks have the same degree of polymerization as the different arms of the heteroarm star.

EXPERIMENTAL PART

Materials

All the polymeric samples involved in this work were synthesized via anionic polymerization under argon atmosphere. A PS/P2VP heteroarm star copolymer designated as PS_6P2VP_6 was prepared according to a three-step sequential 'living' copolymerization method, the details of which are reported elsewhere[18]. A PS/P2VP diblock copolymer, designated as PS-b-P2VP, was synthesized according to standard methods using LiCl in the reaction medium in order to provide low M_W distribution. Both copolymers were purified by dissolving the raw materials in a cyclohexane heptane (95/5 v/v) solvent mixture at room temperature. In this mixture only the linear PS residuals are soluble and can be easily separated from the copolymer by filtration. After several circles the remaining precipitants were redissolved in benzene and freeze dried.

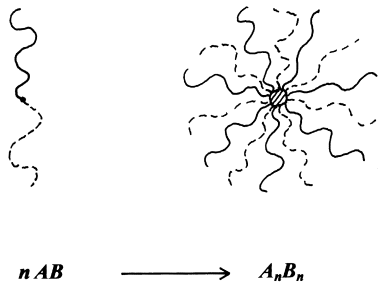

Scheme 1

Characterization of the purified samples was performed by light scattering, gel permeation chromatography, differential refractometry and NMR. All the molecular characteristics are presented in *Table 1*.

Static light scattering

All the light scattering experiments were carried out using a thermally regulated ($\pm$ 0.1°C) spectrogoniometer model SEM RD (Sematech, France) equipped with a He–Ne laser (633 nm). The refractive index increments d*n*/d*c* required the light scattering measurements to be obtained by means of a Chromatic KMX-16 differential refractometer operating at 633 nm.

The polymer solutions were heated at 80°C overnight and allowed to equilibrated at room temperature. Prior to the measurements they were made free from foreign particles by centrifugation and by filtration using filters of 0.45 μm. Both purification methods gave reproducible results in the case of PS_6P2VP_6 but not for the PS-b-P2VP in which the aggregates partially precipitated during centrifugation. In the latter case only filtration was used.

Viscometry

Viscometric measurements were carried out with a Schott–Gerate AVS-300 automated viscosity measuring system using an Ubbelohde-type viscometer immersed in a thermally regulated ($\pm$ 0.05°C) water bath.

Intrinsic viscosities [η] were obtained using Huggins plots according to the equation

$$\eta_i/c = [\eta] + K_H[\eta]^2 c$$

where η_i/c is the reduced viscosity, K_H is the Huggins coefficient and c is the polymer concentration in g cm^{-3}.

Microscopy

To study the morphology of the structures obtained by these star polymers, transmission electron microscopy was used. All the experiments carried out with the help of a JEOL 1200-EX Electron Microscope which was operated at 100 kV. We have studied the morphology in a conventional way (i.e. at room temperature), as well as with help of cryo-electron microscopy (performed at $-$ 176°C). The latter method makes it possible to look at the polymer in the dissolved state.

First, a 0.01 wt% solution of the polymer in toluene (p.a.) was made and kept at room temperature. For the non-cryo experiments normal carbon-coated copper grids were used. A droplet of the solution was put on the grid and subsequently blotted with filter paper. In this way it is

Table 1 Molecular characteristics of copolymers

Sample	$M_w/PS_{arm} \times 10^{-4}$	$M_w/PS_n \times 10^{-4}$	n	$M_w \times 10^{-4}$	W^a_{P2VP} (%)	$M_w/P2VP_{arm} \times 10^{-4}$	M_w/M^d_n
PS_6P2VP_6	2.3	15	6.3	32.9	53.5	2.85[b]	1.12
PS-b-P2VP	2.3		1	4.6	47.0	2.16[c]	1.12

[a] By NMR.
[b] $M_w(P2VP_{arm}) = [M_w(PS_nP2VP_n) - -M_w(PS_n)]/n$.
[c] $M_w(P2VP_{block}) = M_w(PS\text{-}b\text{-}P2VP)\ W_{P2VP}$.
[d] By GPC.

possible to obtain a rather thin film of the polymer of interest. We also performed cryo-electron microscopy to have a direct look at the polymer in solution. The experimental details are described elsewhere[16]. Here we made use of a so-called Controlled Environment Vitrification System (CEVS) to diminish the very fast evaporation of the toluene. The copper grids used are now covered with a holey carbon grid. For this experiment, a 0.02 wt% in toluene was used. Furthermore, the solution was stained with iodine to enhance the contrast.

RESULTS AND DISCUSSION

Static light scattering

In order to evaluate the model of association of the heteroarm star copolymers in a selective solvent, light scattering intensities obtained with different angles and concentrations were treated according to standard procedure[19].

In *Figure 1* the inverse scattering intensity extrapolated to zero angle, $(Kc/\Delta I)_{\Theta=0}$, for the PS_6P2VP_6 is plotted as a function of concentration. As this plot shows, three regions can be distinguished. At low concentrations (region I) $(Kc/\Delta I)_{\Theta=0}$ *versus c* is linear. In this region, single star molecules (unimers) predominately exist and extrapolation to zero concentration gives the inverse molecular weight of the unimer. At high concentrations (region III) the plot is again linear but extrapolation to zero concentration gives much higher molecular weights revealing that the PS_6P2VP_6 star polymers form polymolecular micelles. In this region the equilibrium between micelles and unimers is shifted in favour of micelles and extrapolation to zero concentration can be used to evaluate the degree of association (aggregation number, N_{agg}). At intermediate concentration a transition region (II) exists, characterized by an abrupt decrease in the inverse scattering intensity against *c*. In this region a continuous increase in the number of associating molecules is evident. The regions I and II are separated from each other by a critical concentration, the so-called critical micelle concentration (*cmc*). The plot of *Figure 1* exhibits the concentration dependence corresponding to the 'closed association' model demonstrated schematically in the inset of *Figure 1*.

In an attempt to evaluate the effect of star-shaped architecture on the association phenomena of block copolymers, light scattering measurements were also performed on PS-b-P2VP and the results are incorporated in *Figure 1*. Significant differences of the micellization behaviour have been observed. The *cmc* value for diblock copolymer is far lower than the experimental concentrations used here and cannot be observed by the present experiment. The *cmc* of the star copolymer is 7.4×10^{-4} g cm^{-3}, while that of the linear copolymer is 2.2×10^{-7} g cm^{-3}, three orders of magnitude lower, as estimated below (*Figure 8*).

Comparing the regions III of both samples more differences can be drawn. The inverse molecular weight of the linear copolymer is lower than that of the star copolymer as obtained by extrapolation to zero concentration according to:

$$\frac{Kc}{\Delta I} = \frac{1}{M_w P_\theta} + 2A_2 c \qquad (1)$$

where K is the optical constant, ΔI the difference between the scattering intensity of the solution and that of the pure solvent, P_θ the particle scattering function, M_w the apparent molecular weight of the scattering particles, A_2 the second virial coefficient and c the polymer concentration. Given that the molecular weight of PS_6P2VP_6 is about six times higher than that of the PS-b-P2VP, the degree of association is much lower for the star copolymer.

The angular variation of the inverse scattering intensity is given in *Figure 2*. Distinct angular dependencies of the scattering light for the diblock copolymers at concentrations in region III is seen (*Figure 2b*). The dissymmetry factor *z*, which is the ratio of scattering intensities at 45 and 135°, is close to unity for small particles ($R_g \ll \lambda$) while it takes higher values for large particles ($R_g > \lambda/15$). Since both kinds of micelles have similar size and exhibit radius values lower than $\lambda/15$ (*Table 4*), the angular dependence for the diblock copolymer micelles could be attributed to a broader particle size distribution[20]. This is corroborated from the TEM micrographs.

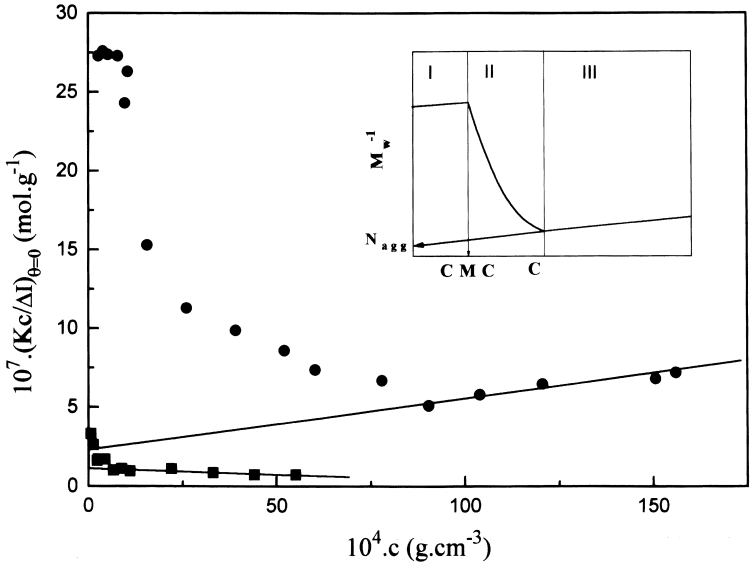

Figure 1 Concentration dependences of $(Kc/\Delta I)_{\Theta=0}$ for PS_6P2VP_6 (●) and PS-b-P2VP (■) in toluene at 25°C. The inset demonstrates the concentration dependence of the inverse apparent molecular weight $(M_{w\ app})^{-1}$ of associating molecules according to the closed association model

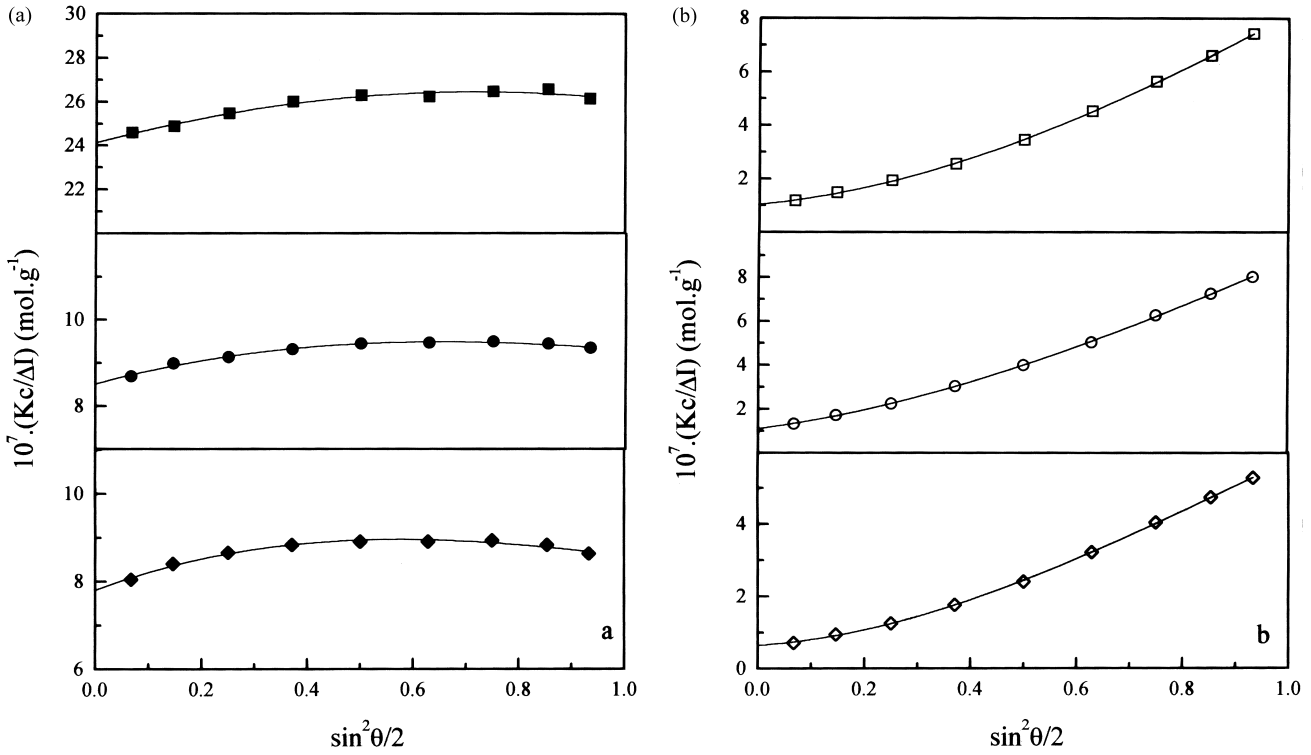

Figure 2 Angular dependence of $Kc/\Delta I$ for (a) PS_6P2VP_6 : (■)12.47 × 10^{-4} g cm^{-3}, (●) 51.9 × 10^{-4} g cm^{-3}, (♦) 104 × 10^{-4} g cm^{-3}; (b) PS-b-P2VP : (□) 8.8 × 10^{-4} g cm^{-3}, (○) 22 × 10^{-4} g cm^{-3}, (◇) 55 × 10^{-4} g cm^{-3}

Differences can also be observed regarding the second virial coefficients A_2 (*Table 2*). The heteroarm star copolymer micelles have a positive value on A_2 while for the micelles constituted from diblock copolymer the A_2 is slightly negative, in agreement with the data reported elsewhere[13,14]. This difference may be attributed to the fact that the corona of the heteroarm star copolymer micelles are constituted of star-shaped polystyrenes for which the solubility is higher compared with the linear homologous. As is known, A_2 for star polymers is higher than the A_2 value of linear ones[21]. The fact that A_2 for the diblock takes a negative value cannot be easily explained since A_2 for the associating systems can be quite complex as it depends on several parameters, such as the interaction of both blocks with the solvent, the molecular weights, the configuration and/or the size of the molecules in solution[22].

A first conclusion that emerges from the comparison of the solution behaviour of the star and linear copolymers is that the influence of architecture on micellization phenomena is quite remarkable. The heteroarm star copolymer micelles exhibit significantly higher *cmc* and lower aggregation number than those formed by diblock copolymers having the same block lengths as the star arms.

The effect of temperature on star micelles was also investigated. Inverse scattering intensities extrapolated to zero angle for the PS_6P2VP_6 in toluene are plotted as a function of concentration for different temperatures in *Figure 3*. As shown, *cmc* is strongly temperature dependent. At 40°C *cmc* is no longer visible as it has been shifted to higher values than the experimental concentrations. The whole concentration region now coincides with regime I (*Figure 1*) implying that the equilibrium has been shifted in favour of unimers. However, at this temperature the diblock copolymers continue to form micelles exhibiting still undetectable low *cmc*. This means that P2VP blocks are insoluble in toluene at this temperature and therefore the heteroarm star copolymers form monomolecular micelles (*Scheme 2*). Obviously the P2VP arms have been collapsed close to the core while the PS arms are swollen from the solvent. This morphology is favoured from the star-shaped architecture, i.e. the radial distribution of the arms which are originating from the star cores. The solubility of these monomolecular micelles is good as is indicated by the high A_2 value (*Figure 3*). Region III is visible at temperatures lower than 30°C and extrapolations to zero concentration coincide indicating that the apparent molecular weight of the micelles is temperature independent.

Table 2 Molecular characteristics of micelles in toluene

Sample	M_w × 10^{-6}	N_{agg}	A_2 × 10^5	R_c^a (nm)
PS_6P2VP_6	4.9	15 ± 1.5	1.5	12 ± 2
PS-b-P2VP	8.9	194 ± 12	−0.03	8.5 ± 2.5

[a]By cryo-TEM.

In order to evaluate the aggregation number of the star micelles we have used the data obtained at 15°C as at this temperature more data can be incorporated to linear regression in regime III. In this regime the equilibrium between micelles and unimers is predominantly in favour of micelles. Assuming that free remaining unimers do not contribute significantly to the scattering intensity and taking into account that the solution of the *cmc* can be considered to be the 'solvent' for the micelles, the data can be analyzed according to the equation[19]

$$\frac{K(c-cmc)}{\Delta I}=\frac{1}{M_wP_\theta}+2A_2(c-cmc) \qquad (2)$$

The *cmc* at 15°C has been evaluated from the logarithm of the *cmc versus* the inverse temperature plot (*Figure 7*). Provided that the d*n*/d*c* values for the PS and P2VP constituents of the copolymer are close to each other,

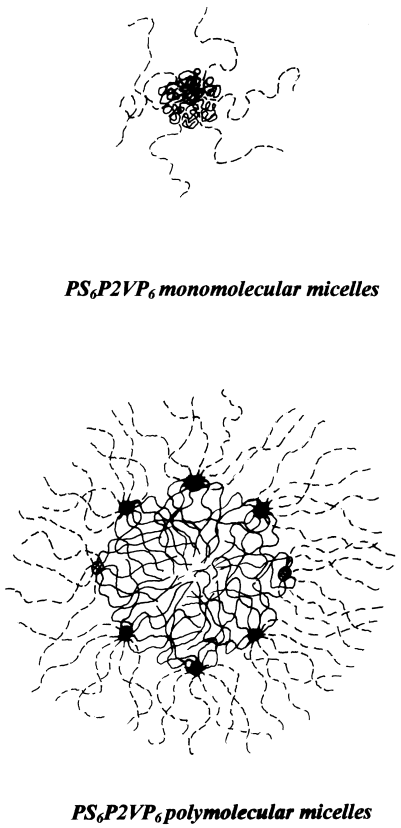

Scheme 2

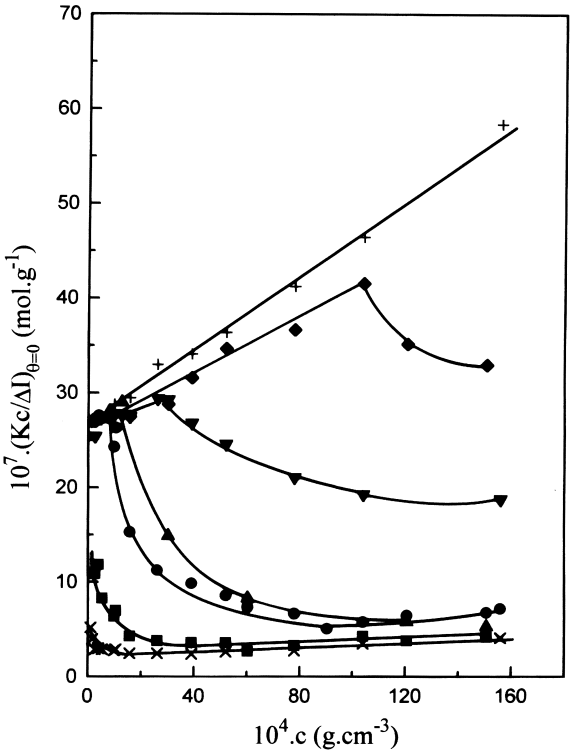

Figure 3 Concentration dependence of $(Kc/\Delta I)_{\Theta=0}$ for PS_6P2VP_6 in toluene at various temperatures : 15 (×), 20 (■), 25 (●), 28 (▲), 30 (▼), 35 (♦), and 40°C (+)

possible compositional heterogeneity does not affect the determination of the true molecular weight of the micelles. The aggregation number, N_{agg}, can thus be estimated by dividing the M_w of the micelle with that of the unimer. All the results concerning the characterization of micelles for PS_6P2VP_6 and PS-b-P2VP are summarized in *Table 2*. Taking into account that each heteroarm star molecule comprises 6.3 PS chains, the number of chains in a polymolecular star micelle is 94, still much lower than N_{agg} of the diblock copolymer micelle.

Morphology

Morphological studies were also performed in the present work by means of transmission electron microscopy. In *Figure 4* an electron micrograph concerning the PS_6P2VP_6–toluene system is illustrated. It is clear from the figure that a number of spherical micelles has been formed. The size distribution is rather small. The dark spheres correspond to the cores of the micelles as the P2VP has been stained with iodine. The average size of the core of the micelles is determined to be 30 nm. However, this result arises from the material which is not in the dissolved state any more. To have a direct look at the micelles solution cryo-electron microscopy was performed. *Figure 5a* shows a cryo-electron micrograph of the solution at −176°C. Clearly the micelles are visible as dark spheres, surrounded by frozen amorphous toluene spanning the small holes in the carbon support film. Some of the micelles are lying on the solid carbon film but are still surrounded by amorphous toluene. Not all the holes are spanned by the solution, which is a normal phenomenon in cryo-electron microscopy. The average diameter of the cores, however, is now somewhat smaller, i.e. 24 nm. This is probably due to the fact that in the first case (*Figure 4*) the micelles are some what flattened

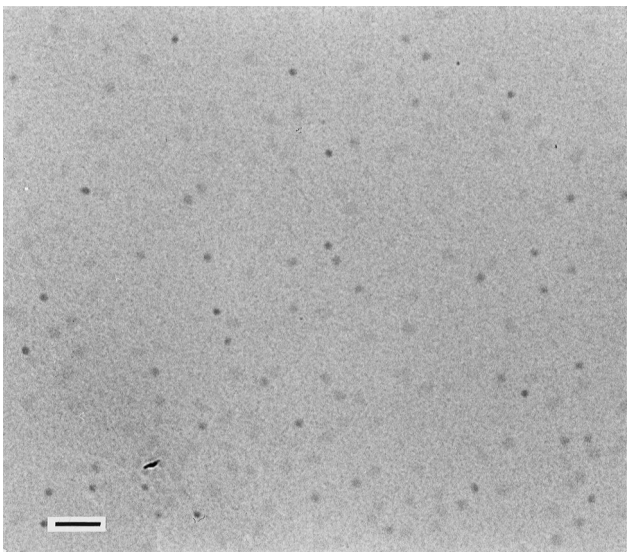

Figure 4 TEM micrograph of PS_6P2VP_6 micelles isolated from a very dilute solution. The scale bar indicates 200 nm

because of the interactions with the carbon support film. Again the size distribution is very small indicating a rather homogeneous association process. From the above standing it is evident for the first time, that the heteroarm star copolymers with nearly symmetrical arm lengths tend to form spherical micelles.

In *Figure 5b* a cryo-electron micrograph of the PS-b-PVP solution is shown. The preparation method was the same as used for the star copolymer in solution. Again, the polymolecular micelles are visible as dark spheres. Actually only one large hole is visible, in contrast to *Figure 5a* where

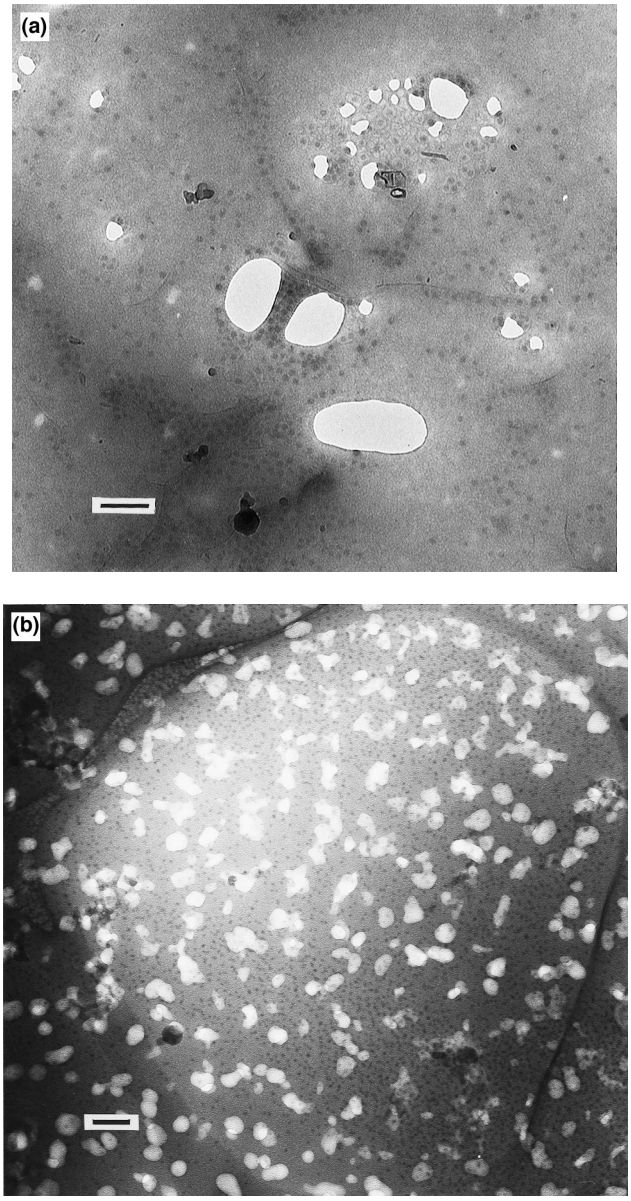

Figure 5 Cryo-electron micrograph of PS_6P2VP_6 (a) and PS-b-P2VP (b) in toluene. The scale bar indicates 200 nm

there are many holes in the carbon support. However, also in this case it is possible to span the hole with the frozen solution. At the edges of the hole the layer is somewhat thicker than in the middle. This is why there are more micelles visible towards the edge. The average value for the diameter is determined to be about 17 nm. This is somewhat smaller than the diameter measured for the star copolymer. The reason will be given in the following.

Thermodynamics of micellization

Provided that the micellization of PS_6P2VP_6 in toluene follows the closed association model, the micelles exhibit a spherical shape of rather small size distribution and the association number is independent of temperature, the thermodynamics of micellization could be investigated[23,24].

As is known for other block copolymer solvent systems undergoing micellization phenomena, the standard Gibbs energy of micellization can be determined using the equation

$$\Delta G^0 = RT \ln(cmc) \tag{3}$$

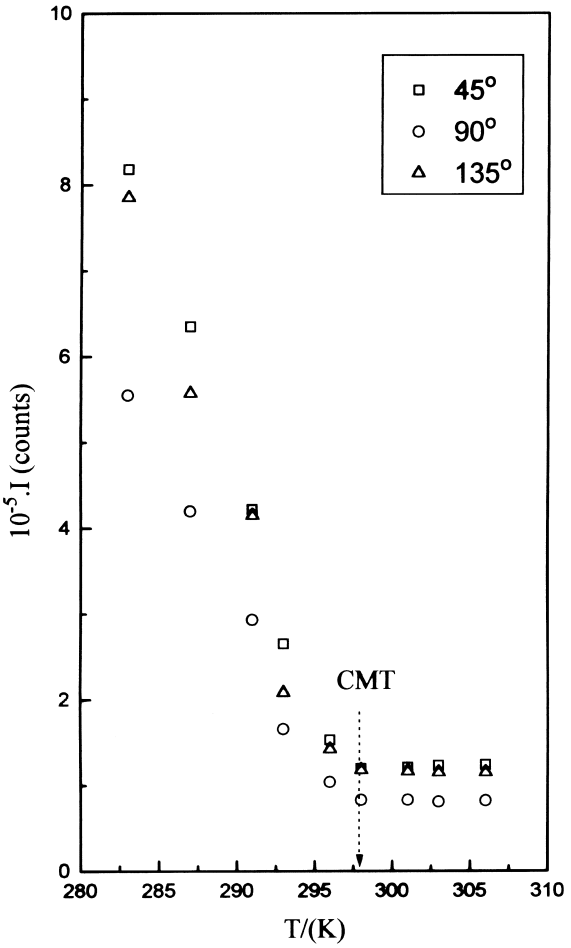

Figure 6 Plot of the light scattering intensity I as a function of temperature at three different scattering angles for the PS_6P2VP_6/toluene system ($c = 0.52 \times 10^{-3}$ g cm^{-3}). The arrow indicates the critical micelle temperature

From the temperature dependence of *cmc*, the standard enthalpy of micellization, ΔH^0, can also be determined using the Gibbs–Helmholtz equation

$$\Delta H^0 = R \frac{\mathrm{d} \ln(cmc)}{\mathrm{d}T^{-1}} \tag{4}$$

Finally, the standard entropy of micellization can be estimated since ΔG^0 values are known at different temperatures, by using the equation

$$\Delta G^0 = \Delta H^0 - T\Delta S^0 \tag{5}$$

An alternative presentation of the light scattering data is to plot the scattering intensities as a function of temperature for a given concentration. From such plots a critical micelle temperature (*cmt*) can be established[25–27]. The *cmt* of a solution of a given *c*, is defined as the temperature at which the appearance of micelles can just be detected experimentally. A representative plot for the determination of *cmt* is illustrated in *Figure 6*. Light scattering intensities at 45, 90 and 135° have been plotted *versus* temperature for the PS_6P2VP_6 at $c = 5.2 \times 10^{-4}$ g cm^{-3} in toluene. The temperature at which the intensity starts to increase abruptly (indicated by the arrow) is considered as the *cmt*. For linear block copolymer micelles in organic solvents it has been shown[28] that within experimental error

$$\frac{\mathrm{d} \ln(cmc)}{\mathrm{d}T^{-1}} = \frac{\mathrm{d} \ln c}{\mathrm{d}(cmt)^{-1}} \tag{6}$$

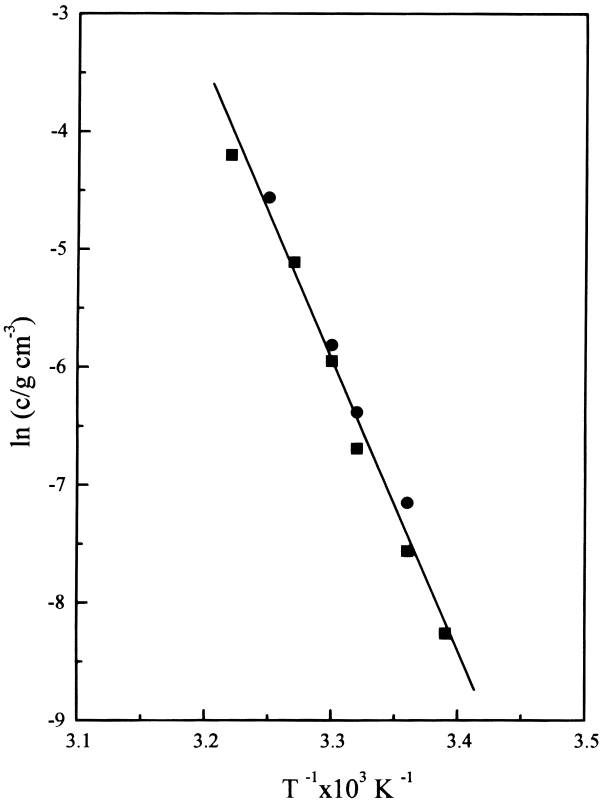

Figure 7 Plot of the logarithm of the concentration as a function of the reciprocal of the absolute temperature for the system PS_6P2VP_6/toluene: (■) ln *cmc versus* 1/*T*, (●) ln *c versus* 1/*cmt*

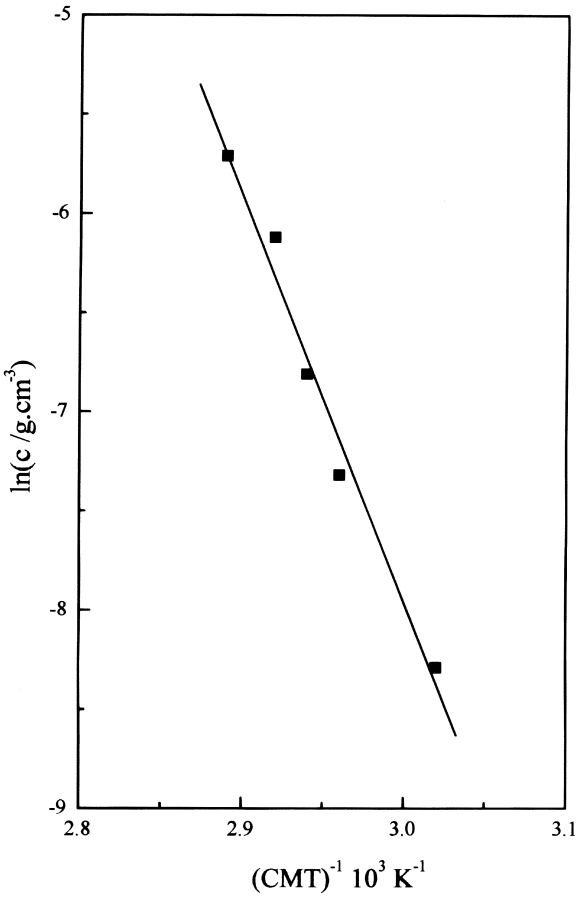

Figure 8 Plot of the logarithm of the concentration as a function of the reciprocal of the critical micelle temperature for the PS-b-P2VP/toluene system

implying that the concentration at which the *cmt* is determined can be considered as the critical micelle concentration at $T = cmt$.

In *Figure 7* ln(*cmc*) for PS_6P2VP_6 in toluene is plotted as a function of the reciprocal of temperature. In the same figure ln *c* is plotted as a function of $(cmt)^{-1}$. As can be seen, all the data lie on a common straight line with a regression factor $r = 0.991$ confirming the validity of equation (6). From this plot, the standard enthalpy of micellization was estimated according to equation (4) and was found to be $-201\ \text{kJ mol}^{-1}$. The negative high value of the standard enthalpy implies that the enthalpy contribution is favourable to micelle formation in agreement with other copolymer/organic solvent systems[23,25–27].

In the case of PS-b-P2VP, only the method based on *cmt* could be applied and at elevated temperatures. In *Figure 8* the plot of ln *c versus* $(cmt)^{-1}$ is linear ($r = 0.99$) and ΔH^0 was found to be $-171\ \text{kJ mol}^{-1}$ as determined by combining equations (4) and (6)

$$\Delta H^0 \approx R\frac{\mathrm{d}(\ln c)}{\mathrm{d}(cmt)^{-1}} \qquad (7)$$

In order to have a better comparison on the thermodynamics of micellization between the linear and star copolymers, ΔG^0 was calculated for both systems and plotted against temperature in *Figure 9*. The standard entropy of micellization, ΔS^0, can be calculated from the slope of the linear fit of ΔG^0 *versus T* plot in accordance with equation (5). All thermodynamic data are listed in *Table 3* and call for some comments.

The micellization free energy values, ΔG^0, for both systems are negative indicating that thermodynamically stable micelles are formed spontaneously. However, for the star copolymer ΔG^0 becomes zero at 83°C and micellization is not favoured at higher temperatures. For the diblock copolymer, this occurs at 143°C.

Table 3 Thermodynamic data[a] for PS_6P2VP_6 and PS-b-P2VP in toluene

Sample	ΔG^0 (T = 25°C) kJ mol^{-1}	ΔH^0 kJ mol^{-1}	ΔS^0 kJ mol^{-1} K^{-1}	T (ΔG^0 = 0) °C
PS_6P2VP_6	−32.6 ± 1.2	−201 ± 8	−0.56 ± 0.02	83
PS-b-P2VP	−47.3 ± 4.2	−166 ± 15	−0.40 ± 0.04	143

[a]The values listed are per mole of copolymer chain.

ΔG^0 is more negative for the diblock copolymer implying a larger driving force for micellization. Analyzing the free energy into the enthalpic and entropic terms it seems that the entropic contribution is responsible for the above mentioned difference. ΔH^0 values for both copolymers are large and negative indicating that the procedure of micellization is an enthalpically favoured process. On the contrary, the standard entropy of micellization is negative showing an unfavourable entropic contribution in agreement with other copolymer/organic solvent systems[23,25–27]. ΔS^0 is more negative for the star copolymer compensating for the benefit of the enthalpic term. The negative value of ΔS^0 is related to a loss of combinatorial entropy as the polymer chains attached to the core are less swollen in the micellar form compared with free chains. It seems that this entropy loss is more pronounced for the copolymer with the star-shaped architecture affecting significantly the micellization thermodynamics of the star copolymer.

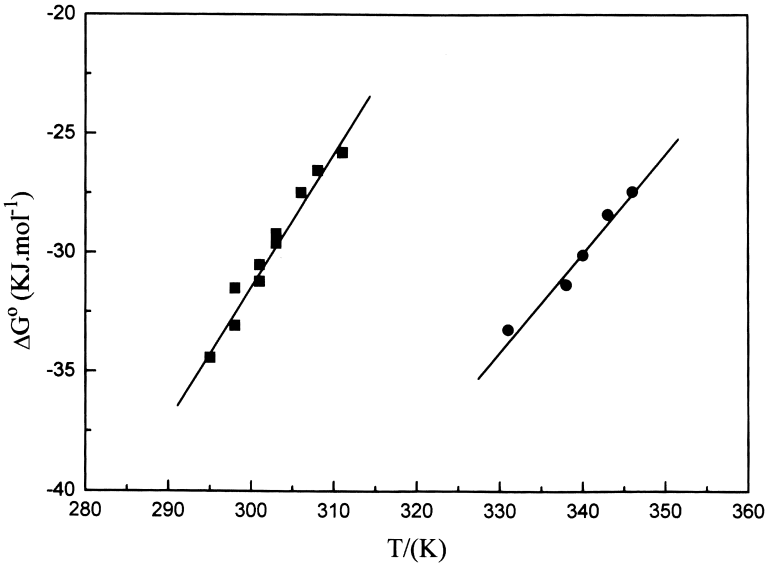

Figure 9 Plot of ΔG^0 of micellization as a function of temperature, for PS_6P2VP_6 (■) and PS-b-P2VP (●) in toluene

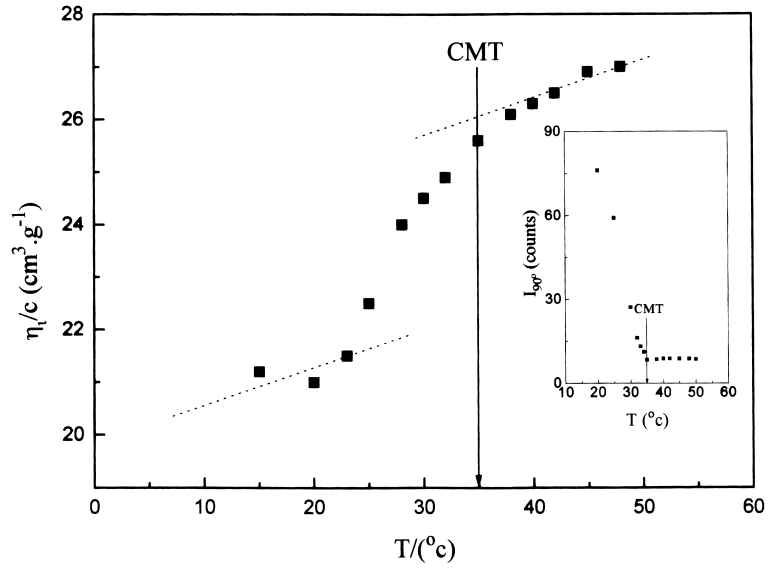

Figure 10 Temperature dependence of the reduced specific viscosity for the PS_6P2VP_6 in toluene. The inset shows the temperature dependence of the light scattering intensity at 90°. Arrows indicate the critical micelle temperature

Viscometry

Viscosity measurements were also employed to characterize the hydrodynamic behaviour of the heteroarm star copolymer micelles. In *Figure 10* the reduced specific viscosity η_i/c of the PS_6P2VP_6 in solution ($c = 1 \times 10^{-2}$ g cm^{-3}) is plotted as a function of temperature. In the inset of this figure the temperature dependence of the light scattering intensity is also illustrated. The viscometric data show a sharp transition, the upper edge of which coincides with the critical micelle temperature. It is obvious that at this concentration, the polymolecular micelles dissociate at higher temperatures leading to monomolecular micelles.

In order to evaluate the hydrodynamic size of the polymolecular and monomolecular PS_6P2VP_6 micelles, intrinsic viscosities $[\eta]$ were determined using the Huggins equation at 20 and 40°C, respectively (*Figure 11*). The concentration range chosen was dictated by the light scattering results demonstrated in *Figure 3*. At 20°C this range corresponds to regime III were the polymolecular micelles predominate while at 40°C this range corresponds to regime I were the star molecules exist in the dissociated form (unimers).

Table 4 Hydrodynamic data of micelles in toluene

Sample	T (°C)	$[\eta]$ (cm^3 g^{-1})	K_H	R_v (nm)
PS_6P2VP_6	20	19.0	0.59	25.0 ± 1.0
	40	22.8	0.63	8.3 ± 0.3
PS-b-P2VP	20	16.0	0.70	28.3 ± 0.5

Intrinsic viscosities for both types of micelles were obtained from the linear extrapolations to zero concentration and are listed in *Table 4*. The $[\eta]$ value at 20°C corresponding to the associated star molecules is very low with respect to their molecular weights, indicating a high compactness of these micelles. This allows us to evaluate the hydrodynamic radius R_v through the model of the hydrodynamically equivalent sphere

$$R_v = \left(\frac{3[\eta]M_w}{10\pi N_A}\right)^{1/3} \quad (8)$$

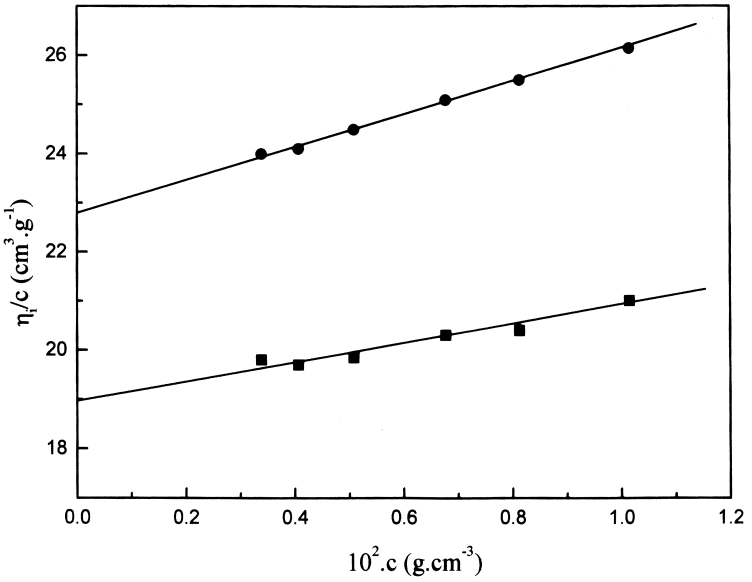

Figure 11 Concentration dependence of the reduced specific viscosity for the PS_6P2VP_6 in toluene at 20 (■) and 40°C (●)

where N_A is the Avogadro number and M_w is the molecular weight of the micelles.

In the case of monomolecular micelles, R_v could be (roughly) evaluated assuming that the hydrodynamic size of the heteroarm star copolymer is determined mainly from the size of the PS star it originated from. As is shown in *Scheme 2* the P2VP arms are in a collapsed state close to the poly(divinyl benzene) core and their contribution to the hydrodynamic volume of the heteroarm star molecule can be considered to be negligible. This idea is corroborated by the fact that the hydrodynamic volume of an A_nB_n heteroarm star polymer remains the same with that of the A_n star polymer it originated from, even in a common good solvent for the A and B arms provided that the length of the B arms is adequately short[4,29]. In this case the Flory equation can be used

$$[\eta] = \Phi(R_v^2)^{3/2}/M_w \quad (9)$$

where Φ is the hydrodynamic constant. It is known that Φ depends on the polymer architecture and, in the case of star-shaped polymers, on the number of arms[30]. The Φ value for a PS star with $n = 6.3$ was taken to be 0.6×10^{25} as evaluated from viscometric data of star PS in toluene[31]. The calculated values of R_v for the star and linear block copolymer are collected in *Table 4*. It seems that the hydrodynamic size of the diblock copolymer micelles is slightly larger than that of the star copolymer micelles.

Since the core radius of the micelles has been determined by cryo-TEM, the corona thickness, L, could be evaluated by subtracting R_c from R_v (*Table 5*). Although the magnitude of L involves rather large errors arising from the fact that R_v and R_c are of different types of averages and that both techniques used for the determination of these averages give remarkable errors, the L values could be used for the sake of comparison.

L for the star copolymer micelles was found to be remarkably lower than that of micelles formed by the linear copolymers, although the polymers used have the same PS chain (block or arm) length. This implies that the corona chains exhibit different conformations for the different micellar systems. The conformation of chains located in the corona is known to be affected by the chain density on the surface of the micelle core keeping all the other factors

Table 5 Corona characteristics of star and linear block copolymer micelles

Sample	L^a (nm)	A_c (nm^2)	$\sigma N_A^{6/5}$	% chain extension
PS_6P2VP_6	13.0	19.1	2.12	23
PS-b-P2VP	19.8	4.7	8.03	36

$^aL = R_v - R_c$.

constant. Eisenberg *et al.*[32,33] have adopted a criterion according to which, if the quantity $\sigma N_A^{6/5}$ becomes greater than 1 the corona chains exhibit a stretched conformation. σ is a dimensionless parameter which has been used to describe the chain density on the surface[34,35] and N_A is the degree of polymerization of the corona chain. σ can be calculated by the equation

$$\sigma = \alpha^2/A_c \quad (10)$$

where α is the length of the repeat unit (0.25 nm for PS) and A_c is the average surface area per corona chains, given from

$$A_c = 4\pi(R_c)^2/N_{agg}f \quad (11)$$

where f is the number of PS arms. Combining equations (10) and (11), $\sigma N_A^{6/5}$ can be rewritten:

$$\sigma N_A^{6/5} = \frac{\alpha^2}{4\pi(R_c)^2} N_A^{6/5} N_{agg} f \quad (12)$$

Since R_c and N_{agg} have been calculated from cryo-TEM and static light scattering respectively, $\sigma N_A^{6/5}$ can be estimated and their values are listed in *Table 5*. In both cases $\sigma N_A^{6/5}$ is greater than unity suggesting that the corona chains exhibit conformations which are extended in the direction perpendicular to the surface in order to accommodate the higher lateral packing of anchored chains at the surface. The value of $\sigma N_A^{6/5}$ for the micelles formed by PS-b-P2VP is greater than that corresponding to the PS_6P2VP_6 micelles implying that the corona chain density is higher in the former case. This suggest that the PS-blocks of the diblock copolymers are in a more stretched form than the PS-arms of the star polymers when located in the corona of the micelle.

An estimation of the degree of chain extension can be

given by comparing the thickness of the corona with the fully extended contour length of the PS chains, i.e. % extension $= 100L/\alpha N_A$ (*Table 5*).

Summarizing the above analysis, we may conclude that the corona of the star copolymer micelles consists of chains with a lower degree of extension than those of micelles formed by linear copolymers due to lower chain density at the surface of the micelle core.

CONCLUSIONS

The association behaviour of heteroarm star copolymers in a selective solvent was investigated by static light scattering, viscometry and cryo-TEM. The system chosen for this study consists of a star polymer bearing nearly symmetrical polystyrene and poly(2-vinyl pyridine) arms (type PS_6P2VP_6) dissolved in toluene which is a selective solvent for PS.

The PS_6P2VP_6 star molecules associate in polymolecular micelles following the closed association model. Static light scattering experiments showed that the plot of the inverse apparent molecular weight *versus* concentration exhibited the ideal concentration dependence and the *cmc* was detectable in the concentration range investigated. The characteristics of the micelles were determined and compared with those of micelles formed by the corresponding diblock copolymers. The effect of architecture on micellization phenomena is significant. The star copolymer micelles exhibit a *cmc* which is three orders of magnitude higher than that of the diblock copolymer micelles. The aggregation number for the PS_6P2VP_6 is one order of magnitude lower than that of the PS-b-P2VP while the size of the micelles shows the opposite trend. Concerning the effect of the macromolecular architecture on N_{agg}, it seems that this is a general trend as other types of branched copolymers (i.e. super-H) show analogous behaviour[36].

The determination of *cmc*'s at different temperatures and *cmt*'s at different concentrations allowed the study and comparison of the thermodynamics of micellization between the two copolymers. In both cases the standard thermodynamic quantities (i.e. ΔG^0, ΔH^0 and ΔS^0) are negative in agreement with the other copolymer–organic solvent systems. However, ΔG^0 for PS_6P2VP_6 becomes positive at temperatures above 87°C where association is not favoured any more. This fact, together with the lower aggregation number and the much higher values of the *cmc*, implies that the heteroarm star copolymers can protect their insoluble parts much easier than the corresponding diblock copolymers exhibiting, therefore, much better solubility.

Finally the combination of the experimental techniques used herein, allowed for elucidation of the structure of the micelles formed by A_nB_n type stars with nearly symmetrical heteroarms. These micelles adopt a core-shell structure of spherical shape with core radius almost equal with the corona thickness (i.e. an intermediate structure between the starlike micelles where $L \gg R_c$ and the crew-cut micelles where $L \ll R_c$ (*Scheme 2*).

Comparing the structural characteristics of the micelles formed by star and/or linear copolymers, we conclude that the star copolymer micelles exhibit a smaller corona thickness with chains which are less stretched with respect to the linear copolymer micelles.

Further work is in progress in an attempt to explore the influence of the molecular characteristics of the heteroarm star copolymers (i.e. number of arms, composition) on the micellization phenomena. Another interesting feature of these star copolymers is that the poly(2-vinyl pyridine) arms can be quaternized yielding star-shaped ionomers. We intend to study these ionomers with this novel architecture in polar and/or non-polar solvents in the near future.

ACKNOWLEDGEMENTS

C.T. would like to thank the Netherlands Foundation for Scientific Research NWO for the financial support of his stay in the University of Groningen.

REFERENCES

1. Bywater, S., *Adv. Polym. Sci.*, 1977, **30**, 89.
2. Roovers, J., Branched polymers, in *Encyclopedia of Polymer Science and Engineering*, Vol. 2, 2nd edition, ed. J. I. Kroschwitz. Wiley-Interscience, New York, 1985, p. 478.
3. Tsitsilianis, C., Chaumont, P. and Rempp, P., *Makromol. Chem.*, 1990, **191**, 2319.
4. Tsitsilianis, C., Graff, S. and Rempp, P., *Eur. Polym. J.*, 1991, **27**, 243.
5. Tsitsilianis, C. and Voulgaris, D., *Macromol. Reports*, 1995, **A32**, 569.
6. Price, C., in *Development in Block Copolymers*, Vol. 2, ed. I. Goodman. Elsevier Applied Science, London, 1985, pp. 27–96.
7. Tuzar, Z. and Kratochvil, P., *Surf. Colloi Sci. Ser.*, 1993, **15**, 1.
8. Reiss, G., Hurtez, G. and Bahadur, P., in *Encyclopedia of Polymer Science and Engineering*, Vol. 2, 2nd edition. Wiley, New York, 1985, pp. 324–434.
9. Alexandridis, P. and Hatton, T. A., *Colloids Surf. A.*, 1995, **96**, 1.
10. Tsitsilianis, C., Papanagopoulos, D. and Lutz, P., *Polymer*, 1995, **36**, 3745.
11. Tsitsilianis, C. and Kouli, O., *Makromol. Rapid Commun.*, 1995, **16**, 591.
12. Star shaped copolymers of the same nature but of different type (PS_2P2VP_1) have also been prepared by using a different synthetic method. Khan, I. M., Gao, Z., Khougaz, K. and Eisenberg, A., *Macromolecules* 1992, **25**, 3002.
13. Sikora, A. and Tuzar, Z., *Makromol. Chem.*, 1983, **184**, 2049.
14. Tang, W.T., Hadziioannou, G., Cotts, P. M. and Smith, B. A., *Polym. Prepr. (Am. Chem. Soc., Div. Polym. Chem.)*, 1986, **27**, 107.
15. Tang, W. T., Ph.D. Thesis, Stanford University, 1987.
16. Oostergetel, G. T., Esselink, F. J. and Hadziioannou, G., *Langmuir*, 1995, **11**, 3721.
17. Esselink, F. J., Semenov, A. N., ten Brinke, G. and Hadziioannou, G., *Macromolecules*, 1995, **28**, 33479.
18. Tsitsilianis, C. and Voulgaris, D., *Macromol. Chem. Phys.*, 1997, **198**, 997.
19. Elias, H.-G., in *Light Scattering from Polymer Solutions*, chapter 9, ed. M. B. Huglin. Academic Press, London, 1972.
20. Tuzar, Z., Sicora, A., Petrus, V. and Kratochvil, P., *Makromol. Chem.*, 1977, **178**, 2743.
21. Roovers, J. E. L. and Bywater, S., *Macromolecules*, 1974, **7**, 443.
22. Khougaz, K., Astafieva, I. and Eisenberg, A., *Macromolecules*, 1995, **28**, 7135.
23. Price, C., Chan, E. K. M., Mobbs, R. H. and Stubbersfield, R. B., *Eur. Polym. J.*, 1985, **21**, 355.
24. Alexandridis, P., Nivaggioli, T. and Hatton, T. A., *Langmuir*, 1995, **11**, 1463.
25. Price, C., Stubbersfield, R. B., El-Kafrawy, S. and Kendall, K. D., *British Polymer J.*, 1989, **21**, 391.
26. Quintana, J. R., Villacampa, M., Munoz, M., Audrio, A. and Katime, I. A., *Macromolecules*, 1992, **25**, 3125.
27. Quintana, J. R., Villacampa, M. and Katime, I. A., *Macromolecules*, 1993, **26**, 601.
28. Price, C., *Pure Appl. Chem.*, 1983, **55**, 1563.
29. Tsitsilianis, C., Kouli O. and Voulgaris D., *6th Polymer Federation Symposium on Polymeric Materials*. Aghia Pelaghia, Crete, Greece, 1996.
30. Roovers, J., Hadjichristidis, N. and Fetters, L. J., *Macromolecules*, 1983, **16**, 214.
31. The Φ value was evaluated by interpolation using values corresponding to 3 and 12 armed-star polymers. Khasat, N., Pennisi, R. W., Hadjichristidis, N. and Fetters, L. J., *Macromolecules* 1988, **21**, 1100.
32. Zhang, L. and Eisenberg, A., *J. Am. Chem. Soc.*, 1996, **13**, 3169.

33. Zhang, L., Barlow, R. J. and Eisenberg, A., *Macromolecules*, 1995, **28**, 6055.
34. Hadziioannou, G., Patel, S., Granick, S. and Tirell, M., *J. Am. Chem. Soc.*, 1986, **108**, 2869.
35. de Gennes, P. G., *Macromolecules*, 1980, **13**, 1069.
36. Iatrou, H., Willner, L., Hadjichristidis, N., Halperin, A. and Richter, D., *Macromolecules*, 1996, **29**, 581.